Usefulness of Volume-rendered Three-dimensional Computed Tomographic Angiography for Surgical Planning in Treating Unruptured Paraclinoid Internal Carotid Artery Aneurysms

MASAMITSU NISHIHARA* and NORIHIKO TAMAKI

Department of Neurosurgery, Kobe University Graduate School of Medicine,

   Paraclinoid internal carotid artery aneurysms are difficult to treat and difficult to visualize by using DSA, MRA, or surface-rendered 3D-CTA. Because those aneurysms are surrounded by bone, the dural ring (proximal and distal), the optic nerve, the oculomotor nerve, and the cavernous sinus. This report represents the first attempt to assess the verification of volume-rendered 3D-CTA for surgical planning in treating paraclinoid internal carotid artery aneurysms. From January, 1996 to October, 2001, we treated 15 cases of unruptured paraclinoid internal carotid artery aneurysms at Kobe University Hospital. Twelve of the patients were women and three were men, ranging age from 33 to 70 (55.7 ± 10.3). We studied used volume-rendered 3D-CTA to examine five patients and surface-rendered 3D-CTA for ten. Volume-rendered 3D-CTA allowed observation of the aneurysms and their necks and the surrounding structures in all cases ($P < 0.001$), while surface-rendered 3D-CTA allowed partial observation of the aneurysms in 5 cases (50%). Volume-rendered 3D-CTA enabled virtual removal of bones by using the clip-plane editing and allowed the aneurysms to be viewed from various angles. When the pterional approach is used and the neck of the aneurysm is found to be remote from the anterior clinoid process, the anterior clinoid process need not be removed. In conclusion, for paraclinoid internal carotid artery aneurysms, volume-rendered 3D-CTA is superior to surface-rendered 3D-CTA, MRA and digital subtraction angiography in terms of visualization of the aneurysm and surrounding bones. It was great help for surgical planning in treating paraclinoid internal carotid artery aneurysms.

   Paraclinoid internal carotid artery aneurysms are difficult to treat. Because those aneurysms are surrounded by bone (the anterior clinoid process), the dural ring (proximal and distal ring), the optic nerve, the oculomotor nerve and the cavernous sinus. In some cases, we need to drill the bone carefully and open the dural ring to see the neck and dome of those aneurysms (4). When the aneurysm is just beside the anterior clinoid process, we should drill the bone carefully not to tear the aneurysm by using the microscope. Among the cerebral aneurysms, a clipping surgery for paraclinoid internal carotid artery aneurysms safely and completely is difficult. The morbidity rates and mortality rates are reportedly high.
   In addition, with paraclinoid internal carotid artery aneurysms it is difficult using the usual radiographic examination techniques - DSA, MRA, and surface-rendered 3D-CTA - to reveal the anatomical relationship between bone and aneurysm, although this relationship is important for surgical planning. Three-dimensional computerized tomographic angiography

Phone: 81-78-382-5966 Fax: 81-78-382-5979 E-mail: nishihara@an.email.ne.jp

(3D-CTA) is useful for the observation of major vessels and bones. But by using surface-rendered 3D-CTA, aneurysms behind bones are difficult to obtain (3). On the other hand, 3D volume rendering takes the entire volume of data, sums the contributions of each voxel along a line from the viewer's eye through the data set, and displays the resulting composite for each pixel of the display (3). According to Villamblanca et al., for the characterization of cerebral aneurysms volume-rendered helical computerized tomographic angiography yields results equal to those obtained with digital subtraction angiography (DSA), and superior to results obtained with magnetic resonance angiography (18). Moreover, because virtual removal of bone is possible with volume-rendered 3D-CTA by using the clip plane and the aneurysms can be easily observed from various angles. The clip plane can be used to interactively "cut away" the objects or other superficial structures to allow visualization of anatomic structures and pathologic conditions within the volume (3).

In this article, we studied the cases of unruptured paraclinoid internal carotid artery aneurysms. We need special effort not to make complications due to surgery because most preoperative symptoms are not serious. Before surgery we should take enough time to reveal the aneurysms and surrounding structure by the radiographic examinations. Once the aneurysms ruptured, emergent surgery is recommended and we should perform examinations immediately without increasing damages. We therefore evaluated, for the first time, the utility of volume-rendered 3D-CTA for surgical planning for unruptured paraclinoid internal carotid artery aneurysms.

MATERIALS AND METHODS

Between January, 1996 and October 2001, we treated 15 cases of unruptured paraclinoid internal carotid artery aneurysms at Kobe University Hospital (Table I). Twelve (80%) of the cases were women and three (20%) were men, with an age distribution ranging from 33 to 70 (55.7±10.3). Eleven of the aneurysms (73.3%) were smaller than 12 mm, and four (26.7%) were larger. Locations of paraclinoid internal carotid artery aneurysms were shown in Table I . The ophthalmic region was 6 cases, the superior hypophyseal region was 6, the ventral region was one, and the carotid cave region was 2.

We examined five patients using volume-rendered 3D-CTA, whereas prior to 1999, we had used surface-rendered 3D-CTA in examining the ten. Helical CT scanners (Somatom Plus 4 Volume Zoom, Siemens Medical Systems, Forchheim, Germany, or High Speed Advantage, GE Medical Systems, Milwaukee, WI) were used (140-200 mA, 120-140 kV). 100 ml (3-4 ml/sec) of contrast material (Iomeron 300, Eisai Co., Tokyo, Japan) was injected intravenously with a 15 to 20 second delay and a reconstruction interval of 0.5 to 1.0 mm. The table speed was 2-4 mm/sec. The scan volume included 20-30 mm above and below the sella turcica. For volume rendering, image analysis was performed using volume-rendering method (3DVirtuoso, Siemens AG, Forchheim, Germany), operating on a Silicon Graphics board (Silicon Graphics, Mountain View, CA). The bone image was visualized in white color (0-1300 Hounsfield Units) and vessels were in red (50-300 Hounsfield Units). The opacity and the brightness were adjusted moderately. The clip planes eliminated the frontal, temporal bone and the anterior clinoid process image. For surface-rendered, image analysis was performed using surface-rendering method (Advantage Windows, GE Medical Systems, Milwaukee, WI). The threshold was from 0 to 200 Hounsfield Units. The anterior clinoid process image was eliminated if possible.

3D Time of Flight SPGR MR angiography sequences (TR 28 msec, TE 6.9 msec, flip angle 20 degree, 256 × 160 matrix, field of view 256 mm) were obtained using 1.5-tesla scanner (Signa Horizon LX, GE Medical Systems, Milwaukee, WI), and the images for all

Table I. Summary of 15 cases of unruptured ophthalmic artery aneurysms.

No	Age/Sex	Side	Region of AN	Size	Symptom	Operation	GOS
1	48/F	R	Ophthalmic	8.5	VFD	Neck clipping	1
2	68/F	L	SH	5	VFD	Neck clipping	1
3	56/F	R	Ophthalmic	23	VFD	Neck clipping, TE	1
4	67/F	L	SH	20	Diplopia*	Neck clipping	1
5	59/F	L	Ophthalmic	16	-	Neck clipping, TE	2(VFD)
6	62/F	R	Ventral	9	-	Neck clipping	1
7	55/M	R	SH	7.5	-	Neck clipping	1
8	67/F	R	Ophthalmic	7.5	-	Neck clipping	1
9	33/F	R	Ophthalmic	10	-	Neck clipping	1
10	56/M	L	SH	12	-	Neck clipping	1
11	46/F	L	Ophthalmic	5	-	Neck clipping	1
12	70/F	L	SH	9.5	VA loss, VFD*	Neck clipping	1
13	49/M	R	SH	5	-	Neck clipping	1
14	46/F	R	Carotid cave	5.5	-	Neck clipping, E	1
15	54/F	R	Carotid cave	7	-	E	1

GOS, Glasgow Outcome Scale; AN, aneurysm; VFD, visual field defect; TE, trapping-evacuation technique; *, postoperative neurological improvement; SH, superior hypophyseal; Size-mm, VA loss, visual acuity loss; E, endovascular treatment.

cases (15 cases) were examined. The whole brain MRA data was acquired 3-4 slabs. The slab thickness was 2.4 cm and divided into 32 partitions.

DSA was performed by using the Seldinger methods and femoral percutaneous catherization (Neurostar, Siemens Medical Systems, Erlangen, Germany). All 15 cases were examined.

The detectabilities of the dome, neck of the paraclinoid internal carotid artery aneurysm, the internal carotid artery, the ophthalmic artery and anterior clinoid process were examined by using surface-rendered 3D-CTA and volume-rendered 3D-CTA. Concerning the visualization of the neck and entire dome of paraclinoid internal carotid artery aneurysms, data were analyzed using the chi-square test. P values of < 0.05 were considered to be significant. The two neurosurgeons assessed the radiographic examinations. The final diagnosis was based on the consensus.

The visualizations of paraclinoid internal carotid artery aneurysms, internal carotid artery, ophthalmic artery and anterior clinoid process were also examined by 3D-CTA, DSA and MRA. All 3D-CTA images were correlated with surgical processes.

RESULTS

Surface-rendered 3D-CTA resulted in partial visualization of the aneurysms in 5 out of 10 cases (50%), while the neck of the aneurysms could not be observed in any of these cases. Volume-rendered 3D-CTA, on the other hand, allowed us to observe in all cases (100%, 5/5)

Table Ⅱ. Visualization by using 3D-CTA.

No	Rendering	Dome	Neck	ICA	Opht
1	SR	-	-	+	-
2	SR	-	-	+	-
3	SR	partial	-	+	-
4	SR	partial	-	+	-
5	SR	partial	-	+	-
6	SR	-	-	+	-
7	SR	-	-	+	-
8	SR	partial	-	+	-
9	SR	-	-	+	-
10	VR	R,whole	R+	+	-
11	SR	partial	-	+	-
12	VR	whole	+	+	-
13	VR	whole	+	+	-
14	VR	R,whole	R+	+	-
15	VR	R,whole	R+	+	-

-, No visualization; +, visible; ICA, internal carotid artery; Opht, ophthalmic artery; R, removal of the anterior clinoid process were needed; SR, surface-rendered; VR; volume-rendered. By using VR 3D-CTA, the entire dome visualized in 5 cases out of 5 cases (P < 0.001, chi-square method), the neck in 5 cases out of 5 cases (P < 0.001, chi-square method).

Table Ⅲ. Visualization of paraclinoid internal carotid artery aneurysms, ICA, Ophthalmic artery, anterior clinoid process (%).

	Dome	Neck	ICA	Opht	ACP
VR	100 (5/5)	100 (5/5)	100 (5/5)	0 (0/5)	100 (5/5)
SR	50 (5/10)	0 (0/10)	100 (10/10)	0 (0/10)	100 (10/10)
DSA	100 (15/15)	100 (15/15)	100 (15/15)	100 (15/15)	0 (0/15)
MRA	100 (15/15)	100 (15/15)	100 (15/15)	100 (15/15)	0 (0/15)

VR, volume-rendered 3D-CTA; SR, surface-rendered 3D-CTA; ICA, internal carotid artery; Opht, ophthalmic artery; ACP, anterior clinoid process.

the aneurysms, the anterior clinoid process, and the ophthalmic segment of the carotid artery and the neck of aneurysms. In three cases, virtual removal of the anterior clinoid process was needed to reveal the entire body of the aneurysm and neck (Table Ⅱ). In two cases, volume-rendered 3D-CTA revealed the neck was away from the bone. A clipping operation was performed without removing the bone in the two cases and intravascular operation was performed in one case. Using surface-rendered 3D-CTA, however the bone images could not be removed without erasing part of the aneurysm images. Consequently, by using surface-rendered 3D-CTA we were not able to produce simulation views for surgery (Table Ⅱ). By using volume-rendered 3D-CTA, the neck was revealed in all cases (P<0.001), that

was statistically significant. The entire dome of the aneurysm was revealed in all cases (P<0.001), that was also significant.

Comparing 3D-CTA with DSA and MRA, the relationship between the anterior clinoid process and aneurysms were not able to be found by using DSA and MRA (0%, 0/15) (Table Ⅲ). The results of the visualization of arteries were shown in Table Ⅲ. By using 3D-CTA, the internal carotid artery was revealed (100%, 15/15), but the ophthalmic artery was not revealed in all cases (0%, 0/15). MRA and DSA were able to visualize the internal carotid artery and the ophthalmic artery in all cases (100%, 15/15).

A clipping operation was performed in 14 cases. Postoperative visual field defect (lower nasal quadrant hemianopsia) and transient hemiparesis appeared in one case each (1/14, 7%). The mortality rate was 0%. Using volume-rendered 3D-CTA, the morbidity and mortality rate was 0% (0/5).
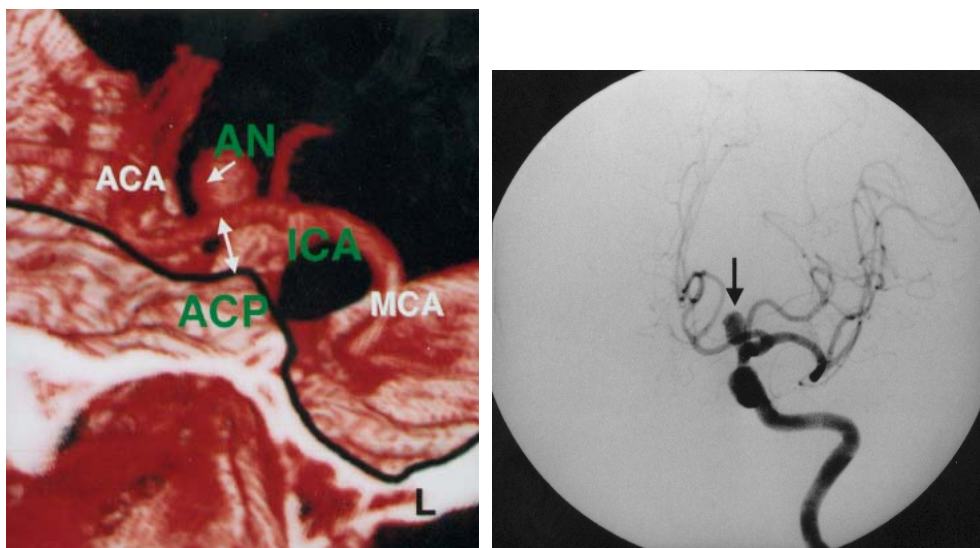

Fig. 1. (a, left) On volume-rendered 3D-CTA, the neck was revealed away from the bone without removal of the anterior clinoid process. A solid line is the edge of bone. (b, right) On left carotid angiogram, the aneurysm projected from the medial wall of the internal carotid artery. The arrow indicates the aneurysm. ICA, Internal carotid artery; AN, Aneurysm; ACP, Anterior clinoid process; ACA, anterior cerebral artery; MCA, Middle cerebral artery.

As a result of the volume-rendered 3D-CTA imaging, paraclinoid internal carotid artery aneurysms could be divided into two types. The first was the aneurysm which was away from the anterior clinoid process and the second was the aneurysm which covered with the anterior clinoid process. We demonstrated the typical cases. The first type was as follows. Volume-rendered 3D-CTA facilitated observation of the aneurysm and its neck from various angles, and clearly showed the space between the aneurysm and the anterior clinoid process (Fig. 1a). In this type, clipping was performed without removal of the anterior clinoid process. On the other hand, the left carotid angiograms showed the aneurysm (Fig. 1b), but that was two-dimensional image and did not give us enough information about the surrounding bone for surgical planning. The second type was as follows. Volume-rendered 3D-CTA identified the location of the aneurysm as just next to the right side of the anterior clinoid process (Fig. 2a), and also showed that, in order to expose the neck during surgery, the anterior clinoid process had to be removed. When the clip plane removed the anterior

clinoid process, the neck of aneurysm became visible (Fig. 2b). Using the left fronto-orbital approach, the anterior clinoid process was drilled carefully while flushing the optic nerve with a generous amount of water. The optic strut and the roof of the optic canal were then removed. After this procedure, the optic nerve was easily mobilized to expose the neck of the aneurysm. The clipping operation was performed without any postoperative neurological deficits. On the other hand, the left carotid angiograms (Fig. 2c) and MRA (Fig. 2d) showed the large aneurysm, but that did not give us enough information about bone.
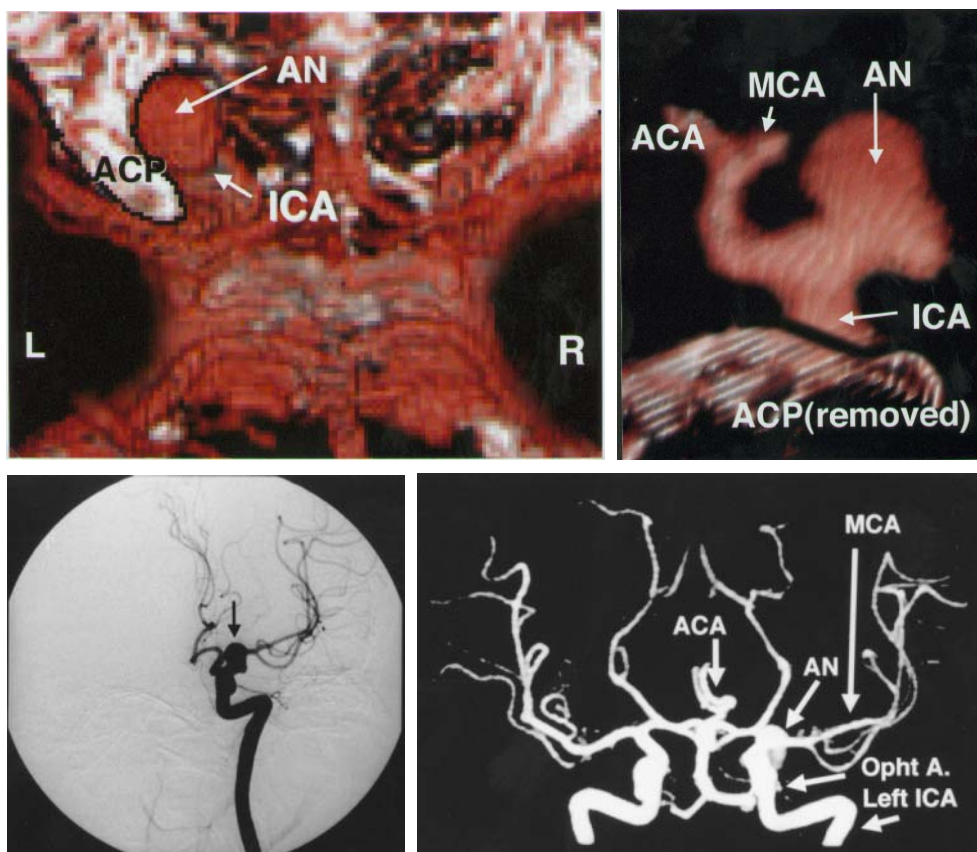

Fig. 2. (a, upper left) On volume-rendered 3D-CTA, a part of the aneurysm is viewed. A solid line is the edge of bone. (b, upper right) On volume-rendered 3D-CTA, the anterior clinoid process is removed by the clip planes. The aneurysm and its neck are demonstrated clearly. A solid line is the edge of bone. (c, lower left) On left carotid angiogram, the aneurysm is revealed (arrow). (d, lower right) On MRA, the aneurysm is demonstrated. But there is no information about bone. ICA, Internal carotid artery; AN, Aneurysm; ACP, Anterior clinoid process; ACA, anterior cerebral artery; MCA, Middle cerebral artery; Opht A, ophthalmic artery.

Surface-rendered 3D-CTA was considered inferior to volume-rendered 3D-CTA for revealing aneurysms in this region. A representative case is as follows. The surface-rendered 3D-CTA demonstrated a part of the aneurysm located behind the anterior clinoid process (Fig. 3a). However the latter procedure did not allow for observation of the neck and body of the aneurysm below the anterior clinoid process, nor of the ophthalmic segment of the carotid artery. DSA showed the aneurysm (Fig. 3b), but that did not give us enough information about bone.
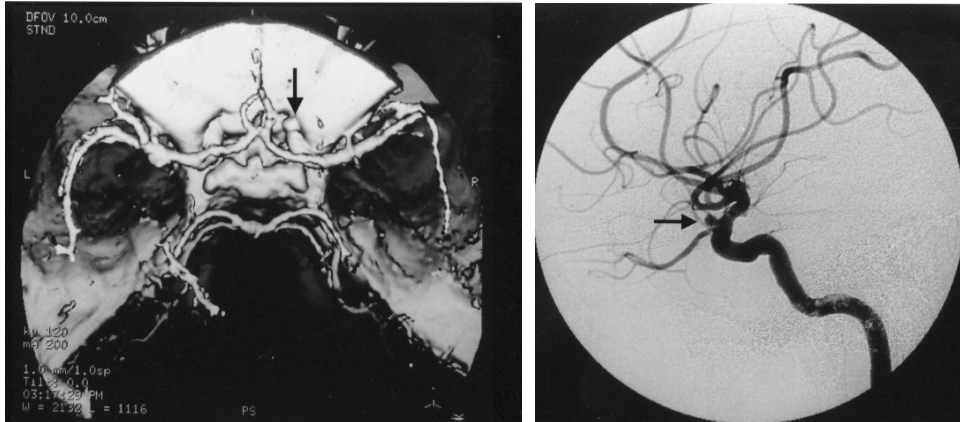
Fig. 3. (a, left) On surface-rendered 3D-CTA, a part of the aneurysm is demonstrated (arrow).
(b, right) On right carotid angiogram, the aneurysm is revealed (arrow).

DISCUSSION

With volume rendering, all voxels within the image volume are available for examination (3). We can change the color of the objects depending on the thresholds. Clip-plane editing can eliminate the objects. Recently, rapid progress has been made in the CPU technology. It takes less than 30 minutes to obtain volume-rendered 3D-CTA, and to obtain the views from various angles, and to remove objects virtually by using the clip-plane editing. In the case of paraclinoid internal carotid artery aneurysms, volume-rendered 3D-CTA can show the relationship of the aneurysm to the surrounding bone, the entire dome ($P < 0.001$) and the neck ($P < 0.001$), and they were statistically significant. Volume-rendered 3D-CTA is supposed to be useful for planning in treating unruptured internal carotid artery aneurysms. When the pterional approach is used and the neck of the aneurysm is found to be remote from the anterior clinoid process, the anterior clinoid process need not be removed. When the anterior clinoid process covers the aneurysm and its neck, the anterior clinoid process can be removed virtually in order to consider of the advisability of clipping. This is great help in surgical planning.

A common criticism of surface rendering is that the surface is derived from only a small percentage (less than 10% by some estimates) of the available data. In addition, surface rendering is not adequate for the visualization of structures that do not have naturally well-differentiated surfaces (3). When surface-rendered 3D-CTA is used, the image of bone and the aneurysm become one and the image of bone cannot be removed without erasing that of the aneurysm. Kogori et al. and other authors reported volume-rendered 3D-CTA was superior to surface-rendered (6,10).

The incidence of paraclinoid internal carotid artery aneurysms has been reported to be 0.5 to 11% of all intracranial aneurysms (4, 20). Paraclinoid internal carotid artery aneurysms arise between the roof of the cavernous sinus and the origin of the posterior-communicating artery. Paraclinoid internal carotid artery aneurysms are surrounded by the anterior clinoid process, the optic nerve, the oculomotor nerve, the dural ring (proximal and distal) and the cavernous sinus. There are many terms for the aneurysms depending on the anatomical landmark: paraophthalmic, supraophthalmic, infraophthalmic, proximal ICA, global, paraclinoid, supraclinoid, subchiasmal, parachiasmal, suprachiasmal, dorsal, ventral, carotid cave, and transitional cavernous aneurysms (4, 9, 14, 19, 20). Assessing the respective anatomical relationships before surgery by using only DSA and MRA is difficult because

there is no information about bone. Therefore, we evaluated, for the first time, the utility of volume-rendered 3D-CTA for surgical planning of paraclinoid internal carotid artery aneurysms. For safe clipping of paraclinoid internal carotid artery aneurysms, it is important to remove the anterior clinoid process, optic canal roof and lateral wall, because extensive removal of the clinoid process exposes the clinoid space and opens the dural ring for excellent exposure of the internal carotid artery and the aneurysm (2, 4). The morbidity rates and mortality rates of paraclinoid internal carotid arteries were reported high in comparison with other cerebral aneurysms. Batjer reported the morbidity rate was 12% (11/89), and the mortality rate was 1% (1/89) (1). Nagasawa reported the morbidity rate was 7% (2/27), the mortality rate was 4% (1/27) (11). In our series, the morbidity rate was 6.7% (1/15), the one case being a visual field defect (lower nasal quadrant hemianopsia) due to injury to the optic nerve. The mortality rate was 0% (0/15). Using volume-rendered 3D-CTA, the morbidity and mortality rates were 0% (0/5). Kumon et al. reported that visual disturbance may result from injury to the ipsilateral optic nerve as a result of excessive retraction, or from the heat of the diamond drill. To prevent such injury, they recommend use of continuous saline drip during drilling of the optic canal, intermittent drilling, and cutting the optic nerve sheath at its lateral border (11). Kakizawa et al. reported an advantage to the contralateral approach in that they were able to preserve visual function (7). Before surgery, volume-rendered 3D-CTA will give us enough information about the contralateral approach. When the aneurysms fall in the large or giant category, the neck is difficult to observe, even virtually, and clipping is considered to be difficult, so that other procedures should be employed. For such cases, we recommend the trapping-evacuation technique that Tamaki et al. reported earlier (17) or retrograde suction decompression of the aneurysm (16).

A limitation of volume-rendered 3D-CTA is that small arteries can not be visualized (18). In our cases, the ophthalmic and superior hypophyseal arteries could not be visualized. The diameter of the internal carotid artery is 4.0-6.5 mm, that of the ophthalmic artery is 1.56 mm, that of the superior hypophyseal artery is 0.2-0.3 mm, and that of the perforators from ICA (ophthalmic segment) is 0.1-0.5 mm (5, 12). In this region, only the internal carotid arteries could be visualized by using 3D-CTA. For viewing the relationship between the aneurysm and the ophthalmic artery, DSA and MRA are superior to 3D-CTA. Kato et al. reported 3D-CTA is a reliable alternative method to conventional angiography in the diagnosis of anterior circulation and most aneurysms of regular size. In such cases it may be possible to obtain the same quality of preoperative information, while being less invasive. Selected cases of ruptured intracranial aneurysms can be successfully managed with the preoperative information provided by 3D-CTA, and without DSA (8, 15). If volume-rendered 3D-CTA visualizes the small arteries, 3D-CTA provides sufficient information and may take the place of DSA in the future.

CONCLUSION

1. Advances in neuroradiology, especially volume-rendered 3D-CTA, have proved useful for visualizing the entire dome of the paraclinoid internal carotid artery aneurysm and neck (they were statistically significant), and surrounding bones. In this respect, volume-rendered 3D-CTA is superior to surface-rendered 3D-CTA, MRA and digital subtraction angiography.
2. When the pterional approach is used and the neck of the paraclinoid internal carotid artery aneurysm is found to be remote from the anterior clinoid process by using volume-rendered 3D-CTA, the anterior clinoid process need not be removed.

REFERENCES

1. **Batjer, H.H., T.A. Kopitnik, C.A. Giller, and D.S. Samson.** 1994. Surgery for paraclinoidal carotid artery aneurysms. J. Neurosurg. **80**:650-658.
2. **Cawley, C.M., G.J. Zipfel, and A.L. Day.** 1998. Surgical treatment of paraclinoid and ophthalmic aneurysms. Neurosurg. Clin. N. Am. **9**:765-83.
3. **Calhoun P.S., B.S. Kuszyk, D.G. Heath, J.C. Carley, and E.K. Fishman.** Three-dimensional Volume Rendering of Spiral CT Data: Theory and Method. 1999. Radiographics **19**:745-764.
4. **Day, A.L.** 1990. Aneurysms of the ophthalmic segment. J. Neurosurgery **72**:677-691.
5. **Gibo, H., S. Kobayashi, K. Sugita, and A.L. Rhoton Jr.** Microsurgical Anatomy of the Supraclinoid Portion of the Internal Carotid Artery and Its Branches 1989. Clinical Anatomy of the Orbit and Its Relations to the Paranasal Sinuses and Optic Nerve. Surgical Anatomy for Microneurosurgery p73-85. In Kobayashi S. (ed.), Tokyo, Japan.
6. **Johnson, P.T., D.G. Heath, D.B. Bliss, B.S. Kuszyk, and E.K. Fishman.** CT angiography with volume rendering: advantages and applications in splanchnic vascular imaging. 1996. Radiology **200**: 564-568.
7. **Kakizawa, K., Y. Tanaka, Y. Orz, T. Iwashita, K. Hongo, and S. Kobayashi.** 2000. Parameters for Contralateral Approach to Ophthalmic Segment Aneurysms of the Internal Carotid Artery. Neurosurgery **47**:1130-1137.
8. **Kato, Y., K. Sano, K. Katada, Y. Ogura, M. Hayakawa, N. Kanaoka, and T. Kanno.** 1999. Application of three-dimensional CT angiography (3D-CTA) to cerebral aneurysms. Surg. Neurol. **52**:113-121.
9. **Kobayashi, S., K. Kyoshima, H. Gibo, S.A. Hegde, T. Takemae, and K. Sugita.** 1989. Carotid cave aneurysms of the internal carotid artery. J. Neurosurgery **70**:216-221.
10. **Kogori Y., M. Takahashi, K. Katada, Y. Ogura, K. Hasuo, M. Ochi, H. Utsunomiya, T. Abe, and S. Imakita.** 1999. Intracranial Aneurysms: Detection with Three-dimensional CT Angiography with Volume Rendering-Comparison with Conventional Angiographic and Surgical Findings. Radiology **211**: 497-506.
11. **Kumon, Y., S. Sakaki, K. Kohno, S. Ohta, S. Ohue, and Y. Oka.** 1997. Asymptomatic, unruptured carotid-ophthalmic artery aneurysms: Angiographical differentiation of each type, operative results, and indications. Surg. Neurol. **48**:465-472.
12. **Lang, J.** 1989. Clinical Anatomy of the Orbit and Its Relations to the Paranasal Sinuses and Optic Nerve. Surgical Anatomy for Microneurosurgery p3-18. In Kobayashi S. (ed.), Tokyo, Japan.
13. **Nagasawa, S., T. Ohta, and E. Tsuda.** 1996. Surgical results and the related topographic anatomy in paraclinoid internal carotid artery aneurysms. Neurol. Res. **18**:401-408.
14. **Nayef, R.F., Al-Rodhan, G.D. Piepgras, and T.M. Sundt Jr.** 1993. Transitional Cavernous Aneurysms of the Internal Carotid Artery. Neurosurgery **33**:993-998.
15. **Ohkawa, M., M. Tanabe, Y. Toyama, N. Kimura, S. Mino, K. Takayama, and G. Satoh.** 1998. CT angiography with helical CT in the assessment of acute stage of subarachnoid hemorrhage. Radiat. Med. **16**:91-97.

16. **Scott, A.J., T.G. Horner, and T.J. Leipzig.** 1991. Retrograde suction decompression of an ophthalmic artery aneurysm using balloon occlusion. J. Neurosurgery **75**:146-147.

17. **Tamaki, N., S. Kim, K. Ehara, M. Asada, K. Fujita, K. Taomoto, and S. Matsumoto.** 1991. Giant carotid-ophthalmic artery aneurysms: direct clipping utilizing the "trapping-evacuation" technique. J. Neurosurgery **74**:567-572.

18. **Villamblanca, J.P., N. Martin, R. Jahan, Y.P. Gobin, J. Franzee, G. Duckwiller, J. Bentson, M. Hardart, D. Coiteiro, J. Sayre, and F. Vinuela.** 2000. Volume-rendered helical computerized tomography angiography in the detection and characterization of intracranial aneurysms. J. Neurosurgery **93**:254-264.

19. **Yasargil, M.G. and J.L. Fox.** 1975. The microsurgical approach to intracranial aneurysms. Surgical Neurology **3**:7-14.

20. **Yasargil, M.G., J.C. Gasser, R.M. Hodosh, and T.V. Rankin.** 1977. Carotid-ophthalmic aneurysms: direct microsurgical approach. Surgical Neurology **8**:155-165.